MicroRNA-21 Aggravates Cyst Growth in a Model of Polycystic Kidney Disease

Ronak Lakhia,* Sachin Hajarnis,* Darren Williams,* Karam Aboudehen,† Matanel Yheskel,* Chao Xing,‡ Mark E. Hatley,§ Vicente E. Torres,‖ Darren P. Wallace,¶ and Vishal Patel*

*Department of Internal Medicine and ‡McDermott Center for Human Growth and Development, University of Texas Southwestern Medical Center, Dallas, Texas; †Department of Internal Medicine, University of Minnesota Medical School, Minneapolis, Minnesota; §Department of Oncology, St. Jude's Children's Research Hospital, Memphis, Tennessee; ‖Departments of Nephrology and Hypertension, Mayo Clinic College of Medicine, Rochester, Minnesota; and ¶Department of Internal Medicine and the Kidney Institute, University of Kansas Medical Center, Kansas City, Kansas

ABSTRACT

Autosomal dominant polycystic kidney disease (ADPKD), one of the most common monogenetic disorders, is characterized by kidney failure caused by bilateral renal cyst growth. MicroRNAs (miRs) have been implicated in numerous diseases, but the role of these noncoding RNAs in ADPKD pathogenesis is still poorly defined. Here, we investigated the role of miR-21, an oncogenic miR, in kidney cyst growth. We found that transcriptional activation of miR-21 is a common feature of murine PKD. Furthermore, compared with renal tubules from kidney samples of normal controls, cysts in kidney samples from patients with ADPKD had increased levels of miR-21. cAMP signaling, a key pathogenic pathway in PKD, transactivated miR-21 promoter in kidney cells and promoted miR-21 expression in cystic kidneys of mice. Genetic deletion of miR-21 attenuated cyst burden, reduced kidney injury, and improved survival of an orthologous model of ADPKD. RNA sequencing analysis and additional *in vivo* assays showed that miR-21 inhibits apoptosis of cyst epithelial cells, likely through direct repression of its target gene *programmed cell death 4*. Thus, miR-21 functions downstream of the cAMP pathway and promotes disease progression in experimental PKD. Our results suggest that inhibiting miR-21 is a potential new therapeutic approach to slow cyst growth in PKD.

J Am Soc Nephrol 27: 2319–2330, 2016. doi: 10.1681/ASN.2015060634

Autosomal dominant polycystic kidney disease (ADPKD), caused by mutations of either *PKD1* or *PKD2*, is among the most common monogenetic disorders and the fourth leading cause of ESRD in the United States. ADPKD is characterized by the presence of innumerable fluid–filled cysts that are lined by epithelial cells.[1,2] The cyst epithelial cells exhibit abnormalities in proliferation, apoptosis, and fluid secretion, which result in the expansion of cysts, eventually causing kidney failure. Aberrant activation of numerous signaling pathways underlies the progression of ADPKD. In particular, cAMP signaling has been shown to play a key role in kidney cyst growth. cAMP levels are increased in ADPKD, and inhibiting this pathway slows cyst growth in both mice and humans.[3–6] However, despite recent progress, the pathogenesis of ADPKD is incompletely understood.

MicroRNAs (miRs) are a class of conserved, small noncoding RNAs that regulates post–transcriptional gene expression.[7] miR biogenesis begins in the nucleus, where RNA-polymerase II–dependent transcription of *miR* gene results in the production of a

Received June 11, 2015. Accepted October 27, 2015.

Published online ahead of print. Publication date available at www.jasn.org.

Correspondence: Dr. Vishal Patel, Department of Internal Medicine/Nephrology, 5323 Harry Hines Boulevard, F5206, Dallas, TX, 75390. Email: Vishald.patel@utsouthwestern.edu

long transcript called primary microRNA (pri-miR). Pri-miRs are processed by enzymes Drosha and Dicer to eventually produce approximately 22-nucleotide-long mature miRs. Nucleotide sequences 2–8 at the 5′ end of a mature miR are collectively referred to as the seed sequence. Watson–Crick base pairing between the seed sequence and complementary sequences located primarily in the 3′ untranslated regions of target mRNAs results in translational repression of the target mRNAs.[8] miRs have been implicated in normal kidney development and the pathogenesis of many kidney diseases, including polycystic kidney disease (PKD).[9–12]

We have previously shown that the miR-17~92 cluster promotes kidney cyst growth.[9] However, whether other miRs also regulate PKD pathogenesis is not known. The goal of this study was to determine whether miR-21, an oncogenic miR,[13,14] modulates cyst growth in ADPKD. We found that miR-21 promotes PKD progression and that the manipulation of miR-21 expression to induce cyst epithelial cell apoptosis may be a novel therapeutic approach for ADPKD.

RESULTS

miR-21 Is Upregulated in PKD

We have previously performed microarrays and identified miRs that are aberrantly expressed in a nonorthologous mouse model of PKD (Ksp/Cre;*Kif3a*$^{F/F}$ mice).[9] Quantitative real-time PCR (qPCR) validation of this dataset revealed that miR-21 was among the most robustly upregulated miRs in 28-day-old *Kif3a* mutant kidneys compared with control kidneys (Figure 1A). Therefore, we decided to study the role of miR-21 in greater detail. We determined whether miR-21 is upregulated in orthologous models of PKD. miR-21 expression was analyzed in 21-day-old Pkhd1/Cre;*Pkd2*$^{F/F}$ (*Pkd2*-knockout [KO]) mice, 10-day-old Ksp/Cre;*Pkd1*$^{F/F}$ (*Pkd1*-KO) mice, two orthologous genetic models of ADPKD, and 28-day-old Ksp/Cre;*Hnf-1β*$^{F/F}$ (*Hnf-1β*-KO) mice, an orthologous model of renal cysts and diabetes. *Pkd1*-KO and *Hnf-1β*-KO mice develop an early-onset and rapidly fatal form of PKD. *Pkd2*-KO mice develop comparatively less aggressive cystic kidney disease and represent a relatively long–lived model of PKD. qPCR analysis revealed that the expression of miR-21 was increased by approximately sixfold in *Pkd2*-KO kidneys, fourfold in *Pkd1*-KO kidneys, and fivefold in *Hnf-1β*-KO kidneys compared with their respective age–matched controls (Figure 1A). Thus, miR-21 upregulation is a common feature of the murine form of PKD.

To determine whether the upregulation of miR-21 is associated with cyst initiation or cyst expansion, we characterized *Pkd2*-KO mice in greater detail. Kidney cysts begin to form at postnatal day (P) 14 in *Pkd2*-KO mice and rapidly expand by P21 and P28 (Supplemental Figure 1A). Compared with kidneys from control mice, expression of miR-21 was increased in kidneys from 21- and 28-day-old *Pkd2*-KO mice but not in kidneys from 14-day old *Pkd2*-KO mice (Supplemental Figure 1B). These results indicate that miR-21 upregulation is associated with cyst expansion rather than cyst initiation.

To determine the specific location of miR-21 expression in cystic kidneys, we performed miR *in situ* hybridization using a locked nucleic acid (LNA) –modified probe against miR-21. Compared with renal tubules in wild-type mice, the expression of miR-21 was elevated in cyst epithelial cells of *Pkd2*-KO mice (Figure 1B). miR-21 expression was not observed in renal tubules of miR-21 KO mice or cyst epithelial cells of *Pkd2*-miR-21 double–KO mice, indicating that the anti–miR-21 LNA probe specifically detects miR-21 (Figure 1B). These results indicate that cysts are the primary source for increased levels of miR-21 in PKD. Next, we used the anti–miR-21 LNA probe to determine miR-21 expression in kidney samples from normal humans and patients with ADPKD (n=4). Compared with renal tubules in normal human kidney samples, miR-21 expression was increased in tubular cysts in kidney samples from patients with ADPKD (Figure 1C). Thus, miR-21 upregulation is also observed in human ADPKD.

cAMP Signaling Pathway Transactivates miR-21 in Kidney Cells

miRs can be upregulated because of increased transcription or enhanced post–transcriptional processing of pri-miR transcripts. We found that expression of pri-miR-21 transcript was increased >2.5-fold in *Pkd2*-KO, *Pkd1*-KO, and *Hnf-1β*-KO kidneys compared with their respective controls (Figure 2, A–C). Thus, increased transcription underlies miR-21 upregulation in mouse models of PKD. In mice, the *miR-21* gene is located within exon 12 of *Vmp1*. However, the expression of *Vmp1* (exons 9 and 10) did not change in *Pkd2*-KO, *Pkd1*-KO, or *Hnf-1β*-KO kidneys compared with their respective controls, suggesting that miR-21 transcription is activated independently of *Vmp1* in cystic kidneys (Figure 2, A–C). To understand the mechanisms by which miR-21 transcription is regulated, we characterized the mouse miR-21 promoter. The promoter for human miR-21 has been mapped,[15] and alignment of this sequence with the mouse genome identified a 419-bp conserved region in intron 10 of *Vmp1* (Figure 2D, Supplemental Figure 2). Incorporation of data from the mouse Encyclopedia of DNA Elements Project revealed that the 419-bp region corresponds to marks of an active promoter in kidney, including the presence of histone H3 lysine 4 trimethylation and histone H3 lysine 27 acetylation, hypersensitivity to DNase I enzyme, and RNA-polymerase II binding (Supplemental Figure 2). To assess functional transcriptional activity, we cloned the 419-bp region in intron 10 of *Vmp1* into a luciferase reporter plasmid. Compared with an empty plasmid, the plasmid containing the putative miR-21 promoter exhibited >200-fold higher luciferase activity in mIMCD3 cells (Figure 2E). Reversing the orientation of this region reduced luciferase activity by >60% (Figure 2E). Taken together, these results indicate that the 419-bp region in intron 10 of *Vmp1* functions as a unidirectional miR-21 promoter in kidney cells.

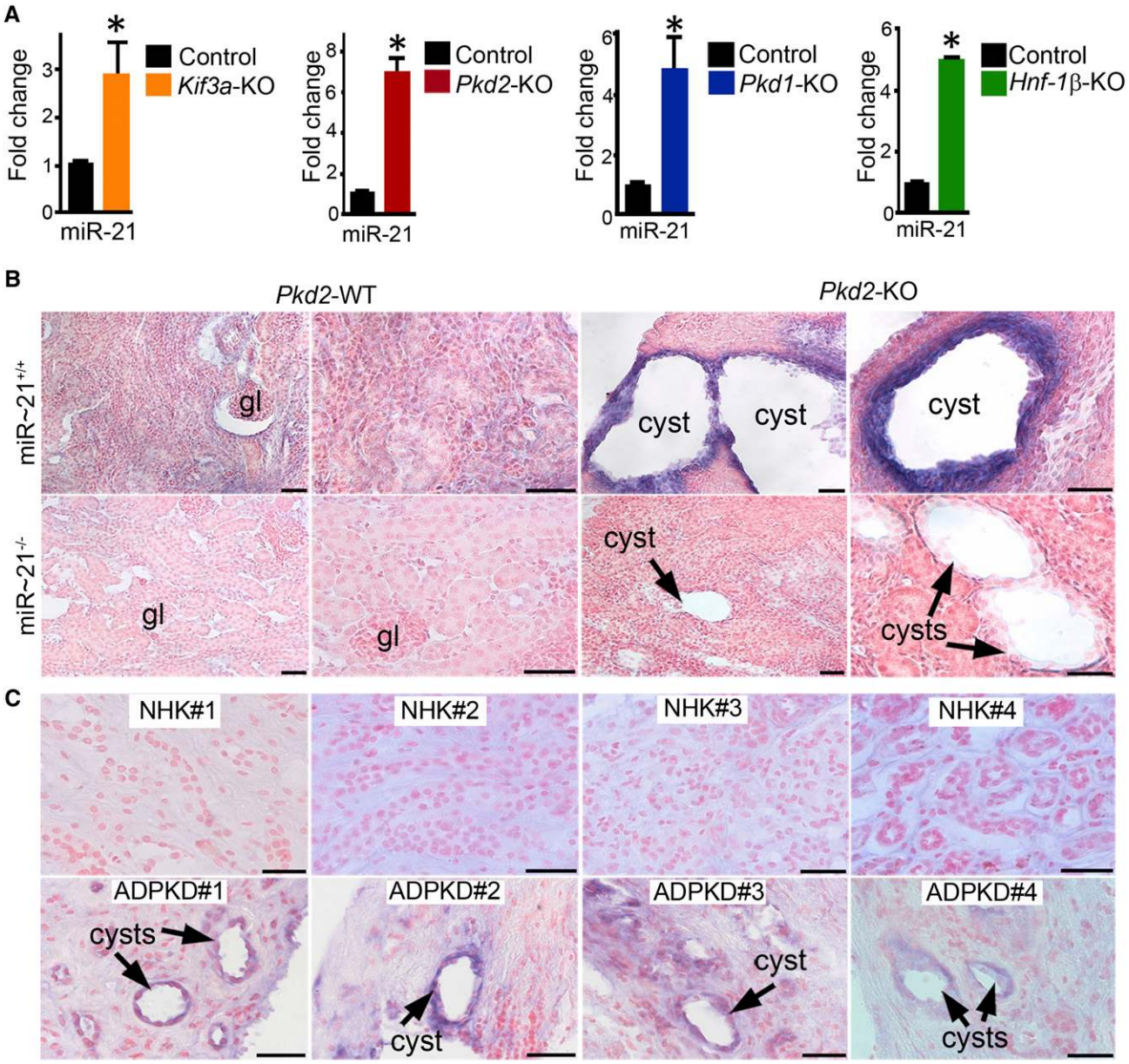

Figure 1. miR-21 is upregulated in PKD. (A) qPCR analysis showing increased expression of mature miR-21 transcript in kidneys of 28-day-old *Kif3a*-KO, 21-day-old *Pkd2*-KO, 10-day-old *Pkd1*-KO, and 28-day-old *Hnf-1β*-KO mice compared with their respective controls (n=3–9 for all groups). *$P<0.05$ (error bars represent SEM). (B and C) *In situ* hybridization (ISH) was performed using an LNA–modified anti–miR-21 probe. The slides were counterstained with nuclear fast red to mark nuclei. (B) Representative ISH images of wild-type, *Pkd2*-KO, miR-21$^{-/-}$, and *Pkd2*-miR-21-KO kidneys are shown. Expression of miR-21 (blue) was increased in cysts of *Pkd2*-KO mice compared with renal tubules of wild-type mice. miR-21 expression was absent in renal tubules of miR-21$^{-/-}$ mice and kidney cysts of *Pkd2*-miR-21-KO mice, indicating specificity of the anti–miR-21 probe. (C) ISH was performed on kidney sections from four different normal human kidney (NHK#1– NHK#4) and ADPKD (ADPKD#1–ADPKD#4) samples. Compared with renal tubules in NHK samples, expression of miR-21 was increased in cysts in kidney samples from patients with ADPKD. gl, Glomerulus; WT, wild type. *$P<0.05$ (error bars represent SEM). Scale bars, 40 μm.

cAMP signaling plays a key role in PKD pathogenesis. cAMP activates protein kinase A (PKA), which in turn, phosphorylates cAMP response element binding protein (CREB) and promotes its transcriptional activity. Bioinformatic analysis revealed that the miR-21 promoter harbors four conserved CREB binding sites, suggesting that cAMP signaling regulates the expression of miR-21. To test this hypothesis, we first determined whether CREB binds to the miR-21 promoter. Chromatin immunoprecipitation (ChIP) was performed using an antibody against CREB and control IgG. Semi-qPCR

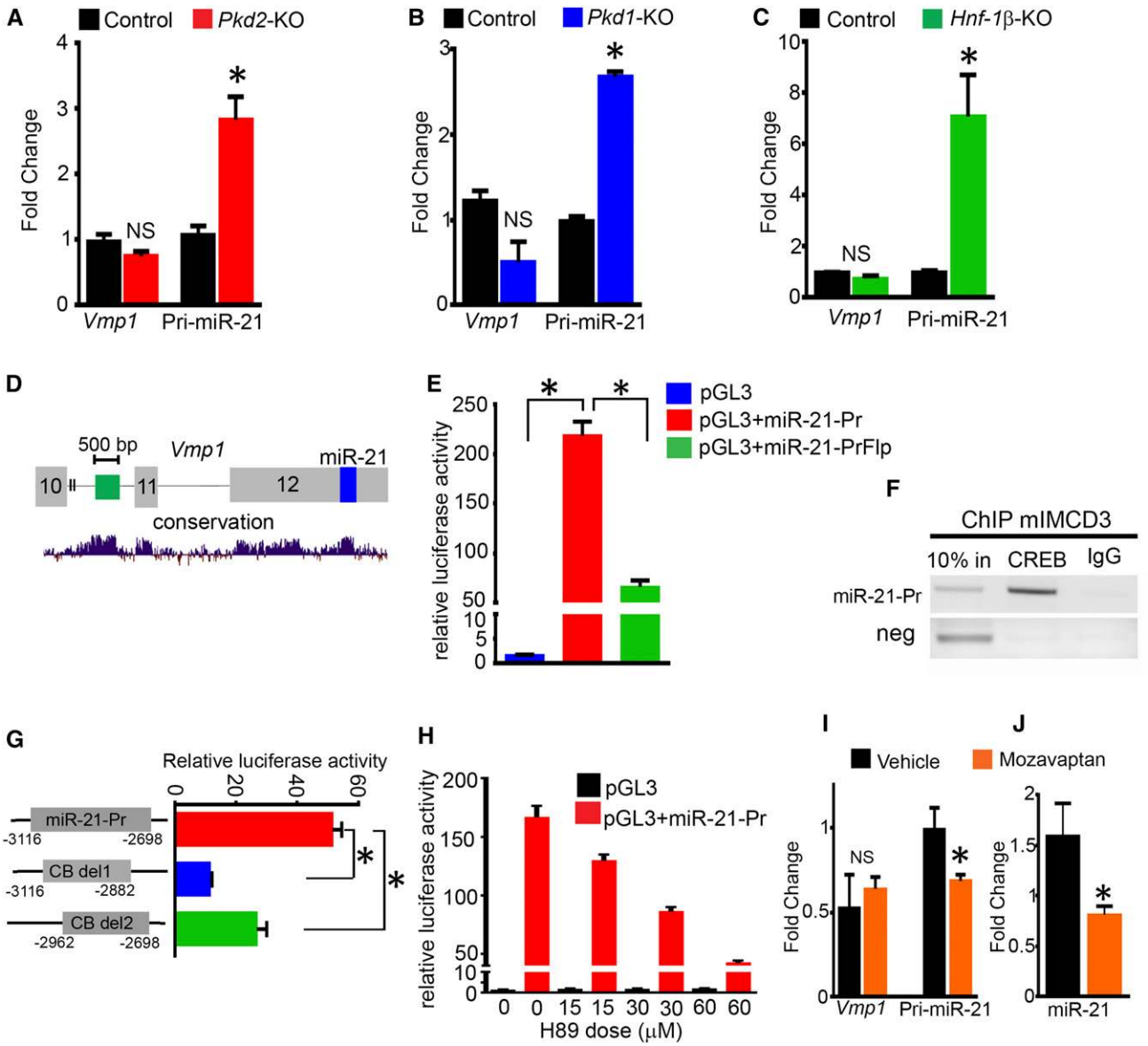

Figure 2. cAMP signaling mediates miR-21 upregulation. qPCR analysis showed that the expression of pri-miR-21 was increased in kidneys of (A) 21-day-old *Pkd2*-KO, (B) 10-day-old *Pkd1*-KO, and (C) 28-day-old *Hnf-1β*-KO mice compared with their respective controls, indicating that transcriptional activation of miR-21 underlies its upregulation in cystic kidneys. In contrast, the expression of *Vmp1* did not change in kidneys of *Pkd2*-KO, *Pkd1*-KO, or *Hnf-1β*-KO mice compared with their respective controls, indicating that miR-21 is activated independently of *Vmp1* in cystic kidneys (n=3–6 for each group). (D) Schematic depiction of genomic organization and cross-species conservation of the miR-21 locus is shown. The mouse miR-21 (blue box) is located in exon 12 (gray box) of *Vmp1*. A 419-bp conserved region (green box) located in intron 10 of *Vmp1* was identified as the putative mouse miR-21 promoter. To assess transcriptional activity, the 419-bp region (green box) was cloned into a pGL3-basic vector to generate pGL3-miR-21-Pr plasmid. The orientation of the region was reversed in pGL3-miR-21-PrFlp construct. (E) Luciferase activity of the indicated pGL3 reporter plasmids in mIMCD3 cells is shown. (F) ChIP was performed using an antibody against CREB and control IgG. Semi-qPCR analysis of the immunoprecipitated DNA revealed that CREB binds specifically to the miR-21 promoter. No PCR product was observed in IgG control. (G) The CREB binding sites in miR-21 promoter were deleted to generate the pGL3+CB-del1 and pGL3+CB-del2 reporter plasmids. CREB binding sites 1 and 2 were deleted in CB-del1 construct, and CREB binding sites 3 and 4 were deleted in CB-del2 construct. Luciferase activity of the indicated pGL3 reporter plasmids in mIMCD3 cells is shown. (H) mIMCD3 cells were transfected with pGL3-miR-21-Pr plasmid and treated with increasing doses of H89 to inhibit PKA activity. Luciferase activity of pGL3-miR-21-Pr plasmid decreased with increasing doses of H89. (I, J) Four-week-old *Pkd2*$^{-/WS25}$ mice were treated with vehicle (n=4) or mozavaptan (n=5), a vasopressin receptor antagonist that decreases renal cAMP levels, for 3 months. *Vmp1* expression was unchanged between the two groups. (I, J) However, the expression of pri-miR-21 and mature miR-21 transcript was significantly decreased in mozavaptan-treated mice compared with vehicle-treated mice. *P<0.05 (error bars represent SEM).

analysis of immunoprecipitated DNA showed enrichment of CREB binding to mouse miR-21 promoter compared with control IgG (Figure 2F). To test whether CREB binding results in functional regulation, we generated luciferase reporter constructs of miR-21 promoter, in which CREB binding sites were deleted. Compared with constructs containing wild-type miR-21 promoter, constructs containing CREB mutant miR-21 promoter displayed decreased luciferase activity in renal epithelial cells (Figure 2G). Thus, CREB binds to miR-21 promoter and regulates its transcriptional activity. Next, we determined whether PKA is needed for miR-21 expression. Administration of H89, a chemical inhibitor of PKA, reduced luciferase activity of miR-21 promoter in mIMCD3 cells (Figure 2H). Taken together, these studies strongly suggest that cAMP signaling directly transactivates miR-21 expression in kidney epithelial cells.

To determine whether cAMP signaling also regulates miR-21 transcription in the context of PKD, we first analyzed miR-21 promoter activity in a previously described *Pkd2*$^{-/-}$ kidney epithelial cell line.[16] Compared with an empty plasmid, the plasmid containing the miR-21 promoter showed >10-fold higher luciferase activity in *Pkd2*$^{-/-}$ cells (Supplemental Figure 3A). Compared with constructs containing wild-type miR-21 promoter, constructs containing CREB mutant miR-21 promoter displayed decreased luciferase activity in *Pkd2*$^{-/-}$ cells (Supplemental Figure 3B). Moreover, administration of H89 also reduced luciferase activity of miR-21 promoter in *Pkd2*$^{-/-}$ cells (Supplemental Figure 3C). Thus, similar to mIMCD3 cells, cAMP also regulated miR-21 promoter activity in *Pkd2*$^{-/-}$ cells. Next, we determined whether cAMP-mediated regulation of miR-21 is observed *in vivo* in cystic kidneys. Four-week-old *Pkd2*$^{-/WS25}$ mice, an orthologous model of ADPKD, were treated for 3 months with either vehicle (n=4) or mozavaptan (n=5). Mozavaptan is a selective vasopressin-2 receptor antagonist that decreases renal cAMP levels and attenuates cyst growth.[17] qPCR analysis revealed that the expression of pri-miR-21 was reduced by approximately 30% (P=0.03) and that the expression of mature miR-21 transcripts was reduced by 50% (P=0.01) in kidneys of mozavaptan–treated *Pkd2*$^{-/WS25}$ mice compared with vehicle–treated *Pkd2*$^{-/WS25}$ mice (Figure 2, I and J). Consistent with the notion that cAMP signaling regulates miR-21 independent of its host gene *Vmp1*, mozavaptan treatment did not affect Vmp1 expression. Collectively, these results suggest that the cAMP signaling pathway promotes miR-21 transcription in the context of PKD.

Deletion of miR-21 Attenuates Cyst Growth in an Orthologous Model of ADPKD

The increased levels of miR-21 in PKD may be functionally significant or simply represent an innocuous correlate of cyst growth. To distinguish between these possibilities, we analyzed mice with gain-of-function and loss-of-function alleles of miR-21 and studied the effects of genetic deletion of miR-21 in a mouse model of ADPKD. Generation of CAG-miR-21 transgenic mice has been previously described.[13] These mice overexpress miR-21 four- to sixfold over normal levels in all tissues, including the kidney. CAG-miR-21 mice are viable, fertile, and born in expected Mendelian ratios. Hematoxylin and eosin staining of kidney sections from 8-week-old CAG-miR-21 mice revealed normal kidney histology (Supplemental Figure 4). Thus, overexpression of miR-21 by itself is not sufficient to produce kidney cysts. Next, we analyzed miR-21$^{-/-}$ mice.[18] miR-21$^{-/-}$ mice are also viable and fertile and exhibit normal kidney histology and function (Supplemental Figure 5). Thus, deletion of miR-21 by itself also does not produce kidney cysts.

To study the role of miR-21 in the context of PKD, we deleted miR-21 in an orthologous mouse model of ADPKD. miR-21$^{-/-}$ mice were bred with Pkhd1/Cre;*Pkd2*$^{F/+}$ transgenic mice. The first and second generation progeny were intercrossed to eventually generate Pkhd1/Cre;*Pkd2*$^{F/F}$;miR-21$^{+/+}$ (*Pkd2*-KO) and Pkhd1/Cre;*Pkd2*$^{F/F}$;miR-21$^{-/-}$ (*Pkd2*-miR-21-KO) mice. qPCR analysis revealed that, compared with control mice, miR-21 expression was increased in *Pkd2*-KO kidneys, whereas its expression was abolished in *Pkd2*-miR-21-KO mice (Supplemental Figure 6A). In contrast, *Pkd2* expression was equally reduced in kidneys of both *Pkd2*-KO and *Pkd2*-miR-21-KO mice compared with control mice, indicating that a similar level of cre-loxP recombination efficiency was observed in *Pkd2*-KO and *Pkd2*-miR-21-KO mice (Supplemental Figure 6B). *Pkd2*-miR-21-KO mice showed reduced cyst growth compared with *Pkd2*-KO (Figure 3A, Supplemental Figure 7). Kidney weight-to-body weight ratio and number of cysts were reduced and overall survival was improved in *Pkd2*-miR-21-KO mice compared with *Pkd2*-KO mice (Figure 3, B–D). Serum creatinine level was numerically lower in 5-month-old *Pkd2*-miR-21-KO mice compared with *Pkd2*-KO mice; however, this difference was not statistically significant (Supplemental Figure 6F) (P=0.07). Expression of renal tubule injury markers, *Kim1* and *Ngal*, was reduced by approximately 50% in *Pkd2*-miR-21-KO kidneys compared with *Pkd2*-KO kidneys (Figure 3, E and F). Analysis of Pkhd1/Cre;*Pkd2*$^{F/F}$;miR-21$^{+/-}$ (*Pkd2*-miR-21-het-KO) revealed that deleting one allele of miR-21 was also sufficient to reduce kidney size and improve survival (Supplemental Figure 8). Thus, deletion of miR-21 attenuates cyst growth in an orthologous mouse model of ADPKD.

miR-21 Promotes Survival of Cyst Epithelial Cells through Inhibition of *Programmed Cell Death 4*

To explore the mechanisms by which miR-21 promotes cyst growth, we performed global gene expression profiling by sequencing mRNA (RNA-Sequencing [RNA-Seq]) from *Pkd2*-KO and *Pkd2*-miR-21-KO kidneys (P21; n=3). Analysis of the RNA-Seq data revealed that 673 protein-coding genes were differentially expressed between the two groups (P<0.05). The differentially expressed genes were further analyzed using the Ingenuity Pathway Analysis software. Functional annotation clustering revealed that cell death and survival were among the top activated cellular functions in *Pkd2*-miR-21-KO kidneys compared with *Pkd2*-KO kidneys (Figure 4A).

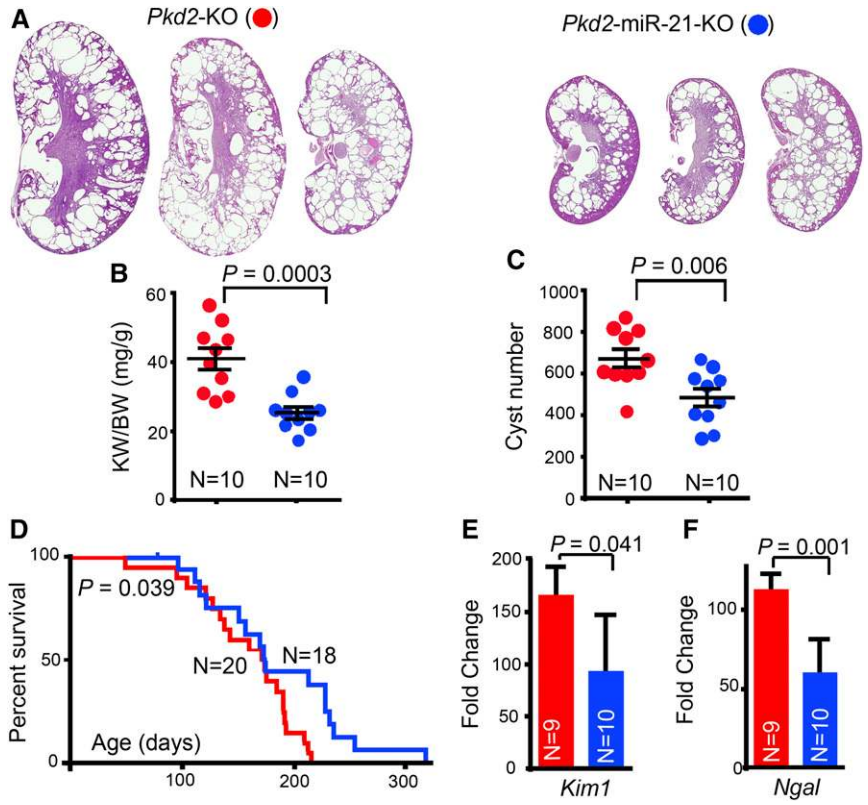

Figure 3. Deletion of miR-21 attenuates cyst growth in an orthologous model of ADPKD. (A) Hematoxylin and eosin staining of kidneys from three different 21-day-old *Pkd2*-KO (left panel) and *Pkd2*-miR-21-KO (right panel) mice is shown. All images were acquired at the same magnification. (B) Kidney weight-to-body weight ratio (KW/BW) and (C) the number of cysts were reduced in *Pkd2*-miR-21-KO mice (blue) compared with *Pkd2*-KO mice (red). (D) Kaplan–Meier survival curves of *Pkd2*-miR-21-KO (blue line) and *Pkd2*-KO (red line) mice. Overall survival of *Pkd2*-miR-21-KO mice was improved compared with *Pkd2*-KO mice (Mantel–Cox log rank, P=0.04). (E and F) qPCR analysis showed that the expression of kidney injury markers *Kim1* and *Ngal* was decreased in kidneys of 21-day-old *Pkd2*-miR-21-KO mice compared with *Pkd2*-KO mice. Error bars represent SEM.

miR-21 is known to inhibit apoptosis and promote survival of malignant cells in various types of cancer.[13,14] Moreover, inducing apoptosis has been shown to slow cyst growth in mouse models of ADPKD.[19] Therefore, we reasoned that deleting miR-21 retards cyst growth by enhancing apoptosis of cyst epithelial cells. We used the terminal deoxynucleotidyl transferase–mediated digoxigenin-deoxyuridine nick–end labeling (TUNEL) assay to detect cyst epithelial cells that were undergoing apoptosis. Kidneys from miR-21$^{-/-}$ mice did not reveal any TUNEL-positive cells, indicating that deletion of miR-21 is not sufficient to induce spontaneous apoptosis of normal kidney cells (Supplemental Figure 9A). In contrast, apoptosis was increased by approximately fivefold in cyst epithelial cells of *Pkd2*-miR-21-KO mice compared *Pkd2*-KO mice, indicating that deleting miR-21 in the context of PKD markedly upregulates apoptosis (Figure 4, B and C). miR-21 is known to promote proliferation, and increased rate of proliferation is thought to underlie cyst growth. Surprisingly, we found that there was no difference in the number of proliferating cyst epithelial cells between *Pkd2*-KO and *Pkd2*-miR-21-KO mice (Supplemental Figure 10, A and B). Furthermore, the expression of proproliferative miR-21 target genes *Cdc25a*, *Cdk2*, and *E2f2* was not different (Supplemental Figure 10, C–E) between *Pkd2*-KO and *Pkd2*-miR-21-KO mice. Thus, deleting miR-21 promotes apoptosis of cyst epithelial cells but does not affect their proliferation.

Next, we identified a direct miR-21 target that may be relevant to apoptosis and kidney cyst growth. *Programmed cell death 4* (*Pdcd4*) is a direct target of miR-21 and a novel tumor suppressor that promotes apoptosis.[20–25] *Pdcd4*$^{-/-}$ mice are born in normal Mendelian ratios and do not exhibit any overt pathology for the first few months of life. However, by approximately 80 weeks, these mice develop abdominal masses, which have been characterized as lymphoma of primary B cell origin. The median lifespan of *Pdcd4*$^{-/-}$ is reduced to 101 weeks compared with the 115- to 150-week lifespan of C57/BL6 mice.[26] Interestingly, in addition to the disseminated lymphoma, approximately 50% of *Pdcd4*$^{-/-}$ mice exhibit multiorgan cysts that involve kidney, ovary, and prostate compared with 14% in the *Pdcd4*$^{+/+}$ littermates. Thus, it is possible that miR-21 promotes cyst growth through direct repression of *Pdcd4*. qPCR analysis revealed that *Pdcd4* expression did not change in miR-21$^{-/-}$ kidneys compared with control kidneys (Supplemental Figure 9B). In contrast, the expression of *Pdcd4* was significantly increased in *Pkd2*-miR-21-KO kidneys compared with *Pkd2*-KO kidneys (Figure 4F). Thus, like apoptosis, miR-21–mediated inhibition of *Pdcd4* expression is also observed in cystic kidneys but not in the normal kidneys. To determine whether miR-21–mediated repression of Pdcd4 occurs in cyst epithelial cells, we stained kidney sections from *Pkd2*-KO and *Pkd2*-miR-21-KO mice with an anti-Pdcd4 antibody. Quantification revealed that the number of Pdcd4–positive cyst epithelial cells was increased more than threefold in *Pkd2*-miR-21-KO mice compared with *Pkd2*-KO mice (Figure 4, D and E). To further examine the miR-21-*Pdcd4*-apoptosis axis in PKD, we analyzed the *Pkd2*-miR-21-Het-KO mice. Compared with *Pkd2*-KO mice, *Pkd2*-miR-21-Het-KO mice also displayed increased apoptosis and enhanced expression of *Pdcd4* (Supplemental Figure 9, C–E). Taken together, these results suggest that miR-21 promotes cyst growth, at least in part, through direct repression of *Pdcd4* in cyst epithelial cells.

A

Molecular and Cellular Function	P-value range	# of molecules
Cell Death and Survival	2.71E-02 - 2.95E-08	118
Cellular Function and Maintenance	2.86E-02 - 2.20E-12	102
Cell to Cell Signaling and Interaction	2.86E-02 - 2.08E-08	101
Cell Morphology	2.86E-02 - 1.86E-08	97
Cellular Compromise	2.32E-02 - 2.95E-08	24

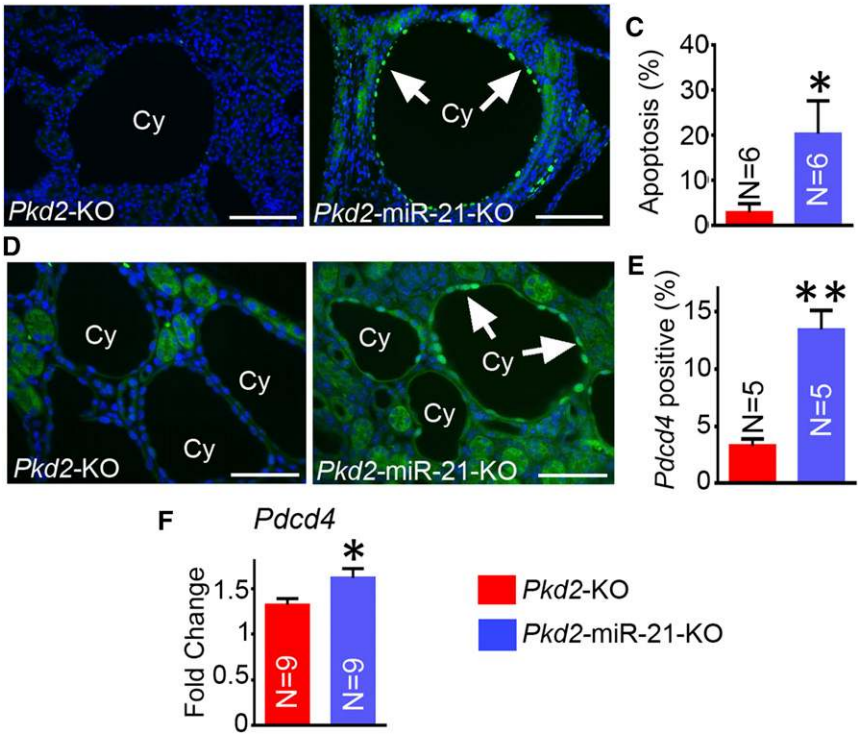

Figure 4. miR-21 promotes survival of cyst (Cy) epithelial cells and inhibits *Pdcd4*. (A) RNA-Seq analysis was performed to identify genes that are differentially expressed in kidneys of 21-day-old *Pkd2*-miR-21-KO mice compared with *Pkd2*-KO mice (n=3). Functional annotation clustering of differentially expressed genes was performed using the Ingenuity Pathway Analysis software. The top five molecular and cellular functions predicted to be changed in *Pkd2*-miR-21-KO kidneys compared with *Pkd2*-KO kidneys are shown. (B) Kidney sections from 21-day-old *Pkd2*-miR-21-KO and *Pkd2*-KO mice were stained using the TUNEL assay to label Cy epithelial cells that were undergoing apoptosis (green with arrows). (C) Quantification of number of Cy epithelial cells undergoing apoptosis in *Pkd2*-miR-21-KO mice compared with *Pkd2*-KO mice is shown. (D) Kidney sections from 21-day-old *Pkd2*-miR-21-KO and *Pkd2*-KO mice were stained with an antibody against Pdcd4 (green with arrows). (E) Quantification of Pdcd4–positive Cy epithelial cells in *Pkd2*-miR-21-KO and *Pkd2*-KO mice is shown. (F) qPCR analysis showing increased expression of *Pdcd4* in kidneys of 21-day-old *Pkd2*-miR-21-KO mice compared with *Pkd2*-KO mice. $^{**}P<0.001$; $^{*}P<0.05$ (error bars represent SEM).

DISCUSSION

Our work suggests that miR-21 is a novel regulator of PKD pathogenesis. As a first line of evidence, we show that miR-21 is upregulated in PKD and that cAMP signaling drives miR-21 expression in cystic kidney. miR-21 is upregulated in non-orthologous rat models of PKD[27]; however, its expression in orthologous mouse model of ADPKD was not known.[28] Moreover, the specific location within the cystic kidney that contributes to elevated levels of miR-21 was also not known. We characterized multiple commonly used mouse models of PKD, including orthologous genetic models of ADPKD, and found that miR-21 upregulation is a common feature of murine PKD. *In situ* hybridization revealed that cyst epithelial cells were the primary source for increased miR-21 levels in cystic kidneys. Furthermore, we found that miR-21 levels were also increased in cysts in kidney samples from patients with ADPKD. Consistent with our findings, miR expression profiling has shown that miR-21 levels are increased in cells originating from cysts of end stage human ADPKD kidneys.[29] Thus, collectively these observations strongly suggest that miR-21 upregulation is a common feature of both rodent and human forms of PKD.

Deregulated expression of multiple miRs is observed in PKD,[9,27–30] but the underlying mechanisms are not well understood. Depending on the disease process, miR-21 can be upregulated because of either increased transcription or enhanced post–transcriptional processing of pri-miR-21 transcripts.[31,32] We found that transcriptional activation was the major cause for miR-21 upregulation in the context of PKD. In humans, miR-21 is located on chromosome 17q23.2 immediately downstream of the protein-coding gene, *VMP1*. miR-21 has been found to be generated through two independently regulated transcripts in human cancer cell lines.[15,33] The first transcript (VMP1-miR-21) is an alternatively spliced *VMP1* transcript that originates at exon 1 of *VMP1* and ends downstream of miR-21. This transcript is regulated through the *VMP1* promoter. The second transcript originates at intron 10 of *VMP1* and is regulated through a unique miR-21 promoter located in the intron 10 of *VMP1*. The relative contribution of the *VMP1*-dependent or *VMP1*-independent mechanisms to the final mature miR-21 transcript levels varies on the basis of the type of tissue/cells or the disease state. We found that the expression of *Vmp1* was not increased in cystic kidneys, suggesting that, in the context of PKD, miR-21 is regulated independently of *Vmp1*. The unique miR-21 promoter that regulates miR-21 expression independently of

VMP1 has been mapped in human cancer cell lines. However, the orthologous mouse miR-21 promoter was poorly characterized. Alignment of the human miR-21 promoter sequence with the mouse genome identified an evolutionarily conserved region in intron 10 of *Vmp1* gene. We confirmed that this region possesses the various hallmarks of a promoter that is transcriptionally active in the kidney, including the ability to drive unidirectional luciferase activity in kidney cells. Activated cAMP-CREB signaling is a key pathologic feature of PKD. Interestingly, the miR-21 promoter harbors four conserved CREB-binding sites. Moreover, in human glioblastoma cell lines, CREB small interfering RNA treatment decreases miR-21 expression.[34] However, whether CREB directly regulates miR-21 promoter activity is not known. We have determined that CREB physically binds to the miR-21 promoter in mouse kidney cells, and mutating CREB binding sites or inhibiting cAMP signaling reduces the transcriptional activity of miR-21 promoter. Furthermore, we found that inhibiting cAMP signaling also inhibits miR-21 expression in a mouse model of ADPKD. Thus, collectively, our data strongly suggest that the cAMP-CREB pathway directly promotes miR-21 transcription in the context of PKD.

As a second line of evidence, we show that inactivation of miR-21 attenuates disease progression in an orthologous mouse model of ADPKD. These results directly implicate miR-21 in pathogenesis of PKD. miR-21 has emerged as a novel drug target for diseases that produce kidney fibrosis.[11,35–37] Anti–miR-21 drugs have been developed, and planning for clinical trials to evaluate safety and efficacy of these drugs in patients with Alport syndrome is underway. Our studies provide genetic proof of principle for preclinical testing of these anti–miR-21 drugs as a new therapeutic approach for PKD. An anti–miR-21 drug could potentially complement and even have unique advantages over the currently available treatment strategies. In addition to the cAMP pathway, many other cyst–promoting signaling pathways (*e.g.*, Jak/Stat and MAP/extracellular signal–regulated kinase) are known to regulate miR-21 expression.[13,38,39] Therefore, downregulation of miR-21 could collectively inhibit the pathogenic effects of multiple cyst–promoting signaling cascades. Although mozavaptan treatment reduces miR-21 expression, it does not completely inhibit its expression. Thus, it is possible that cotreatment with mozavaptan (or tolvaptan) and anti–miR-21 drugs will have synergistic therapeutic effects. Anti-miRs have a long duration of action (as long as 4 weeks). Thus, these drugs may need to be administered once every 3–4 weeks as opposed to the current therapeutic strategies that involves taking medications once or twice daily.

Finally, we provide a potential cellular and molecular mechanism by which miR-21 may aggravate cyst growth. miR-21 is known to inhibit apoptosis, particularly in the context of various cancers.[13,14] Consistent with its antiapoptotic role, deleting miR-21 evoked marked apoptosis of cyst epithelial cells. In contrast, the number of proliferating cyst epithelial cells was not different between *Pkd2*-KO and *Pkd2*-miR-21-KO mice, suggesting that miR-21 deficiency slows cyst growth specifically by inducing apoptosis. Although miR-21 is predicted to target hundreds of mRNAs, inhibition of only a subset of these targets is likely to underlie apoptosis of cyst epithelial cell and cyst growth. Our data suggest that *Pdcd4* could be one such PKD–relevant miR-21 target. Inactivation of miR-21 resulted in increased expression of Pdcd4 in cyst epithelial cells, suggesting that miR-21 inhibits *Pdcd4* in cystic kidneys. There is compelling evidence already showing that *Pdcd4* is a proapoptotic gene and a direct target of miR-21 in cancer. In response to a variety of stimuli, *Pdcd4*-null tissues and cells exhibit reduced apoptosis.[23,40] miR-21 physically interacts with an evolutionarily conserved site in the 3′ untranslated region of *Pdcd4* and inhibits its expression.[13,41] A subset of $Pdcd4^{-/-}$ mice spontaneously develops kidney cysts,[26] suggesting that miR-21–mediated inhibition of *Pdcd4* is a plausible mechanism to aggravate cyst growth. However, our studies provide only correlative evidence in support of the miR-21-*Pdcd4*-apoptosis axis as a pathogenic mechanism for cyst growth. Whether *Pdcd4* inhibition aggravates cysts growth or re-expression of *Pdcd4* attenuates cyst growth in a model of PKD needs to be experimentally validated in future studies. Furthermore, the cystic phenotype of $Pdcd4^{-/-}$ mice is late onset and not fully penetrant. Therefore, inhibition of *Pdcd4* by miR-21 cannot fully explain the severe and fully penetrant cystic phenotype of *Pkd2*-KO mice. Analysis of the RNA-Seq data identified nine additional putative targets of miR-21 in cystic kidneys (Supplemental Table 1). Thus, miR-21 likely aggravates cyst growth through regulation of many other targets genes other than *Pdcd4*.

Our studies suggest a new therapeutic approach for PKD that involves manipulating miR function to induce apoptosis of cyst epithelial cells. Accumulating evidence suggests that stimulating targeted apoptosis of cyst epithelial may have beneficial effects. Treatment with either rapamycin[42,43] or Sirtuin 1 inhibitors[44] inhibits proliferation and induces apoptosis of cyst epithelial cells, which collectively reduce cyst growth in models of ADPKD. Recently, Fan *et al.*[19] showed that directly stimulating apoptosis of cyst epithelial cells, without affecting their proliferation, is sufficient to slow cyst enlargement. Second Mitochondrial Activator of Caspases is a key molecule that promotes apoptosis by repressing the function of Inhibitor of Apoptosis proteins. Treatment with a Second Mitochondrial Activator of Caspases–mimetic drug did not affect proliferation but triggered approximately fourfold more apoptosis of cyst epithelial cells, which in turn, slowed cyst enlargement.[19] These observations provide support for our conclusion that elevated apoptosis of cyst epithelial cells is a potential mechanism by which miR-21 deficiency slows cyst growth. However, the beneficial effects of inducing apoptosis of mutant cyst epithelia could be easily counterbalanced by the deleterious effects of inducing apoptosis of surrounding normal renal tubules. A distinctive feature of miR-21 expression in cystic kidneys is that it is primarily upregulated in the cyst epithelial cells but not in the surrounding normal tubules.

Therefore, inhibiting miR-21 may represent a unique opportunity to target cyst epithelial cells. In contrast to observations made by our group and Fan *et al.*,[19] inhibiting apoptosis has also been shown to slow cyst growth.[45,46] These studies were performed in nonorthologous rodent models that more closely resemble the autosomal recessive form of PKD, whereas the work of our group and Fan *et al.*[19] was performed in orthologous models of ADPKD. The differences in animal models may partly help explain the divergent results. Moreover, ADPKD models exhibit none to very low levels of apoptosis[47]; thus, basal apoptosis is unlikely to be a major contributor of cyst growth in these models.

In conclusion, we have shown that miR-21 is a direct downstream transcriptional target of cAMP signaling and that its expression is increased in cystic kidneys. Upregulation of miR-21 aggravates cyst growth, in part, by inhibiting apoptosis and promoting the survival of cyst epithelial cells. A potential mechanism by which miR-21 promotes cyst epithelia survival may be through direct repression of *Pdcd4*. Our results suggest a novel mechanism involving miRs and regulation of proapoptotic genes in the pathogenesis of kidney cyst growth. Our work also suggests that inhibiting miR-21 may represent a new therapeutic approach for PKD.

CONCISE METHODS

Mice

Pkd2$^{F/F}$,[48] *Pkd1*$^{F/F}$,[47] *Hnf-1β*$^{F/F}$,[49] *Kif3a*$^{F/F}$,[50] miR-21$^{-/-}$,[18] CAG-miR-21,[13] Pkhd1/Cre,[51] Ksp/Cre,[52] and *Pkd2*$^{WS25/-}$[53] mice were used in this study and have been previously described. Equal numbers of male and female mice were included in the analyses shown in Figure 3 and Supplemental Figure 5. Mice were anesthetized under approved protocols, blood was obtained by cardiac puncture, and the right kidney was flash frozen for molecular analysis. The left kidneys was perfused with cold PBS and 4% (wt/vol) paraformaldehyde and then harvested. Kidneys were fixed with 4% paraformaldehyde for 2 hours and then, embedded in paraffin for sectioning. Sagittal sections of kidneys were stained with hematoxylin and eosin for additional analysis. Cyst index and cyst number calculations were performed using ImageJ analysis software as previously described.[9] Serum creatinine was measured using capillary electrophoresis; BUN, aspartate aminotransferase, and alanine aminotransferase were measured using the Vitros 250 Analyzer. Four-week-old *Pkd2*$^{WS25/-}$ mice were treated with either mozavaptan (OPC31260) or vehicle for 3 months; 0.1% OPC31260 was added to ground rodent chow (LaDiet 5053). At 16 weeks of age, mice were anesthetized, and left kidneys were harvested for molecular analysis. All animal studies were approved by the Institutional Animal Care and Use Committees at the University of Texas Southwestern, the Mayo Clinic, and St. Jude's Children's Research Hospital.

Human Specimens

Frozen ADPKD and normal human kidney specimens were provided by the PKD Research Biomaterials and Cellular Models Core at the Kansas University Medical Center (KUMC). ADPKD kidneys were obtained with the assistance of the KUMC Bio-Specimen Repository Core. Kidneys were immediately sealed in sterile bags, submerged in ice, and delivered to the laboratory. Normal kidneys unsuitable for transplantation were obtained from the Midwest Transplant Network (Kansas City, KS). The protocol for the use of surgically discarded kidney tissues complies with federal regulations and was approved by the Institutional Review Board at the KUMC.

In Situ Hybridization

Mouse kidneys were perfused with 4% paraformaldehyde and then, submersed in 30% sucrose overnight followed by freezing with optimal cutting temperature compound; 10-μm frozen sections were obtained and immersed overnight in 10% neutral buffered formalin. The next day, sections were washed with PBS three times and then, treated with proteinase K for 10 minutes at 37°C. Subsequently, Exiqon miRCURY LNA ISH FFPE Protocol (Exiqon miRCURY LNA ISH Optimization Kit 2 #90002) was followed with the following optimization steps. Hybridization temperature of 53°C was used for mouse tissue, and 55°C was used for human samples. Anti–Digoxigenin-AP Fab fragment antibody was used at 1:800 dilution (11093274910; Roche, Basel, Switzerland), and AP substrate was reapplied after 1 hour. Slides were counterstained with nuclear fast red and then, mounted with Eukitt mounting medium. Samples were allowed to settle overnight and then, examined using light microscopy.

ChIP

ChIP assay was performed using the EZ ChIP Kit (EMD Millipore, Billerica, MA) according to the manufacturer's instructions using mIMCD3 cells. Briefly, cells were cross-linked with 1% formaldehyde for 15 minutes at room temperature. Chromatin samples were extracted and sonicated; 5 μg either rabbit anti-CREB1 (sc-186; Santa Cruz Biotechnology, Santa Cruz, CA) or rabbit IgG (sc-2027; Santa Cruz Biotechnology) was used for immunoprecipitation. Genomic DNA was purified and amplified using the following primer set: forward 5′-ACA TCC ATC ATA AGC CAT GAA-3′ and reverse 5′-TTA TCC AAA AAG AAT GCA TTA GCA-3′. The primer set used as a negative control consisted of forward 5′-ACA GGA CGA TGA GTC TGA GTG A-3′ and reverse 5-′ TGT GAC TGT TAG CTG AGC CAT T-3′. The PCR product was subsequently visualized on 1% agarose gel for quantification using 1% of input DNA for normalization.

qPCR

Total kidney RNA was extracted using the Qiagen miRNeasy RNA Extraction Kit (Qiagen, Germantown, MD). cDNA synthesis was performed using an iScript cDNA Synthesis Kit or a Universal cDNA Synthesis Kit from Bio-Rad (Hercules, CA) or Exiqon, respectively. qPCR was performed using SybrGreen from Bio-Rad, Taqman from Life Technologies (Carlsbad, CA), or ExiLent SYBR Green from Exiqon. The following primers sequences were used: miR-21, Exiqon #204230; pri-miR-21, Life Technologies #4427012; *Pkd2*-forward-5′-CAC GAC AAT CAC AAC ATC C-3′; *Pkd2*-reverse-5′-GCG TGG TAC CCT CTT GGC AGT T-3′; *Havcr*-forward 5′-AGC AGT CGG TAC AAC TTA AAG G-3′; *Havcr*-reverse-5′-AGA GTT CTC TAT CGT CAA GGA CA-3′; *Lcn2*-forward 5′-GCA GGT GGT ACG

TTG TGG G-3′; *Lcn2*-reverse-5′-CTC TTG TAG CTC ATA GAT GGT GC-3′; *Pdcd4*-forward 5′-ATG GAG GCC GTC TTA AAC CT-3′; *Pdcd4*-reverse 5′-TGC CTT GTA CCC AAA ACA AA-3′; *Vmp1*-forward (exon 9) 5′-CTG TTT GAC CTG GCT GGA ATA-3′; *Vmp1*-reverse (exon 10) 5′-CAA TGA AAG TCA CCA TCT GCT C-3′; *Cdc25a*-forward 5′-ACA GCA GTC TAC AGA GAA TGG G-3′; *Cdc25a*-reverse 5′-GAT GAG GTG AAA GGT GTC TTG G-3′; *Cdk2*-forward 5′-CCT GCT TAT CAA TGC AGA GGG-3′; *E2F2*-forward 5′-ACG GCG CAA CCT ACA AAG AG-3′; and *E2F2*-reverse 5′-GTC TGC GTG TAA AGC GAA GT-3′.

RNA Sequencing

Strand–specific RNA-Seq libraries were prepared using the TruSeq Stranded Total RNA LT Sample Prep Kit from Illumina. After quality check and quantification, libraries were sequenced at the University of Texas Southwestern McDermott Center using a Hiseq2500 Sequencer to generate 51-bp single-end reads. Before mapping, reads were trimmed to remove low-quality regions in the ends. Trimmed reads were mapped to the mouse genome (mm10) using TopHat versioin 2.0.12 with the UCSC iGenomes GTF file from Illumina.[54] Alignments with mapping quality <10 were discarded. Expression abundance estimation and differential expression gene identification were done using edgeR[55] or Cuffdiff version 2.2.1.[56] Genes with a P value <0.05 were deemed significantly differentially expressed between the two conditions.

Plasmid Construction

The putative miR-21 promoter was PCR amplified using forward and reverse primers that introduced *Mlu*I and *Xho*I restriction sites at the 5′ and 3′ ends, respectively. The sequences of primers were 5′-TAGAATACGCGTGGCAAACATCCATCATAAGC-3′ and 5′-TAGAATCTCGAGAGAGCCACTGCTATGTCAGGA-3′, where the underlined sequences are *Mlu*I and *Xho*I sites, respectively. The 419-bp PCR product was ligated into a pGL3-Basic Plasmid (Promega, Madison, WI) that was previously digested with both *Mlu*I and *Xho*I to generate the pGL3+miR-21-Pr construct. Additional plasmids were constructed using the same cloning strategy. The primer sequences for the various constructs are as follows: pGL3+miR-21-Prflp: forward primer 5′-TAGAATCTCGAGGGCAAACATCCATCATAAGC-3′ and reverse primer -5′-TAGAATACGCGTAGAGCCACTGCTAGTCAGGA-3′ (the underlined sequences are *Xho*I and *Mlu*I sites, respectively); pGL3-CB-del1: forward primer 5′-TAGAATACGCGTGGCAAACATCCATCATAAGC-3′ and reverse primer 5′-TAGAATCTCGAGGAAACTGCCCTCCCTCTCTC-3′ (the underlined sequences for pGL3-A and pGL3-B plasmids are *Mlu*I and *Xho*I sites, respectively); and pGL3-CB-del2: forward primer 5′-TAGAATACGCGTGGACTTAGATTGAGAAAGCACCTC-3′ and reverse primer 5′-TAGAATCTCGAGAGAGCCACTGCTATGTCAGGA-3′ (the underlined sequences for pGL3-A and pGL3-B plasmids are *Mlu*I and *Xho*I sites, respectively). The sequences of all constructs were verified by Sanger sequencing.

Luciferase Reporter Assays

mIMCD3 cells and *Pkd2*$^{-/-}$ cells[16] (gift from Stefan Somlo) were plated in six-well plates (2×10^5 cells per well) and cotransfected with 0.6 μg pGL3 plasmids encoding Photinus luciferase and 0.02 μg pRL-CMV vector encoding the Renilla luciferase. The cells were incubated with increasing amounts of H89 (0, 15, 30, and 60 μM or 0, 5, 10, and 15 μM) for 16 hours and harvested 48 hours post-transfection in 250 μL passive lysis buffer; 30 μL each sample lysate was added into a 96-well plate, and the Photinus and Renilla luciferase activities were measured using the Dual Luciferase Reporter Assay System (Promega) according to the manufacturer's directions. All experiments were performed at least three times in triplicates unless otherwise noted.

TUNEL and Immunofluorescence Staining

TUNEL assay was performed using the Promega Dead End Tunel Flourometric System Kit per the manufacturer's directions with the following modification: the proteinase K treatment time was extended to 15 minutes. The following antibodies were used on paraffin-embedded sections for immunofluorescence staining: phosphohistone H3 (1:400; H0412; Sigma-Aldrich, St. Louis, MO), Pdcd4 (1:300; 9535S; Cell Signaling Technology, Danvers, MA), and Alexaflour goat anti–rabbit 488 (1:500; a11070; Invitrogen, Carlsbad, CA).

Apoptosis and Proliferation Index

Quantification was performed by randomly selecting 10 ×20 magnification fields per sample and subsequently determining the percentage of positively stained cyst epithelial cells. The person performing the quantification was blinded to genotype of kidney sections.

Statistical Analyses

Data shown are means±SEMs. The significance of differences between the means was calculated using the t test. ANOVA was used for multiple comparisons followed by the Dunnett test to detect differences between specific pairs of groups. Log-rank (Mantel–Cox) test was the *a priori* planned comparison for survival differences, which reflects the total survival experience; $P<0.05$ was considered statistically significant.

Accession Codes

The RNA-Seq data are available from the Gene Expression Omnibus under accession number GSE69556.

ACKNOWLEDGMENTS

We thank Peter Igarashi for guidance and support during the course of this project, Eric Olson for helping with planning the initial stages of this study and providing the miR-21$^{-/-}$ mice, and Stefan Somlo for providing *Pkd1*$^{F/F}$ and *Pkd2*$^{F/F}$ mice. We also thank Beverly Huet for statistical analysis. We thank the University of Texas Southwestern O'Brien Kidney Research Core Center, the Yale Center for Polycystic Kidney Disease Research, the McDermott Center Sequencing and Bioinformatics Core, and University of Texas Southwestern Metabolic Phenotyping Cores for providing critical reagents and services.

R.L. is supported by Institutional National Institutes of Health Training Grant T32-DK007257. The Polycystic Kidney Disease Research Biomaterials and Cellular Models Core at the University of Kansas Medical Center is supported by a grant from the Polycystic Kidney Disease (PKD) Foundation (to D.P.W.). Work from the

authors' laboratory is supported by National Institute of Diabetes and Digestive and Kidney Diseases Grants R03 DK099568-01 (to V.P.) and R01 DK102572 (to V.P.) and a grant from the PKD Foundation (to V.P.).

DISCLOSURES

None.

REFERENCES

1. Patel V, Chowdhury R, Igarashi P: Advances in the pathogenesis and treatment of polycystic kidney disease. *Curr Opin Nephrol Hypertens* 18: 99–106, 2009
2. Torres VE, Harris PC, Pirson Y: Autosomal dominant polycystic kidney disease. *Lancet* 369: 1287–1301, 2007
3. Torres VE, Chapman AB, Devuyst O, Gansevoort RT, Grantham JJ, Higashihara E, Perrone RD, Krasa HB, Ouyang J, Czerwiec FS; TEMPO 3:4 Trial Investigators: Tolvaptan in patients with autosomal dominant polycystic kidney disease. *N Engl J Med* 367: 2407–2418, 2012
4. Gattone VH 2nd, Wang X, Harris PC, Torres VE: Inhibition of renal cystic disease development and progression by a vasopressin V2 receptor antagonist. *Nat Med* 9: 1323–1326, 2003
5. Grantham JJ: 1992 Homer Smith Award. Fluid secretion, cellular proliferation, and the pathogenesis of renal epithelial cysts. *J Am Soc Nephrol* 3: 1841–1857, 1993
6. Wallace DP: Cyclic AMP-mediated cyst expansion. *Biochim Biophys Acta* 1812: 1291–1300, 2011
7. Mendell JT, Olson EN: MicroRNAs in stress signaling and human disease. *Cell* 148: 1172–1187, 2012
8. Bartel DP: MicroRNAs: Target recognition and regulatory functions. *Cell* 136: 215–233, 2009
9. Patel V, Williams D, Hajarnis S, Hunter R, Pontoglio M, Somlo S, Igarashi P: miR-17~92 miRNA cluster promotes kidney cyst growth in polycystic kidney disease. *Proc Natl Acad Sci U S A* 110: 10765–10770, 2013
10. Patel V, Hajarnis S, Williams D, Hunter R, Huynh D, Igarashi P: MicroRNAs regulate renal tubule maturation through modulation of Pkd1. *J Am Soc Nephrol* 23: 1941–1948, 2012
11. Patel V, Noureddine L: MicroRNAs and fibrosis. *Curr Opin Nephrol Hypertens* 21: 410–416, 2012
12. Noureddine L, Hajarnis S, Patel V: MicroRNAs and polycystic kidney disease. *Drug Discov Today Dis Models* 10: e137–e1743, 2013
13. Hatley ME, Patrick DM, Garcia MR, Richardson JA, Bassel-Duby R, van Rooij E, Olson EN: Modulation of K-Ras-dependent lung tumorigenesis by MicroRNA-21. *Cancer Cell* 18: 282–293, 2010
14. Medina PP, Nolde M, Slack FJ: OncomiR addiction in an in vivo model of microRNA-21-induced pre-B-cell lymphoma. *Nature* 467: 86–90, 2010
15. Ribas J, Ni X, Haffner M, Wentzel EA, Salmasi AH, Chowdhury WH, Kudrolli TA, Yegnasubramanian S, Luo J, Rodriguez R, Mendell JT, Lupold SE: miR-21: An androgen receptor-regulated microRNA that promotes hormone-dependent and hormone-independent prostate cancer growth. *Cancer Res* 69: 7165–7169, 2009
16. Grimm DH, Cai Y, Chauvet V, Rajendran V, Zeltner R, Geng L, Avner ED, Sweeney W, Somlo S, Caplan MJ: Polycystin-1 distribution is modulated by polycystin-2 expression in mammalian cells. *J Biol Chem* 278: 36786–36793, 2003
17. Torres VE, Wang X, Qian Q, Somlo S, Harris PC, Gattone VH 2nd: Effective treatment of an orthologous model of autosomal dominant polycystic kidney disease. *Nat Med* 10: 363–364, 2004
18. Patrick DM, Montgomery RL, Qi X, Obad S, Kauppinen S, Hill JA, van Rooij E, Olson EN: Stress-dependent cardiac remodeling occurs in the absence of microRNA-21 in mice. *J Clin Invest* 120: 3912–3916, 2010
19. Fan LX, Zhou X, Sweeney WE Jr., Wallace DP, Avner ED, Grantham JJ, Li X: Smac-mimetic-induced epithelial cell death reduces the growth of renal cysts. *J Am Soc Nephrol* 24: 2010–2022, 2013
20. Afonja O, Juste D, Das S, Matsuhashi S, Samuels HH: Induction of PDCD4 tumor suppressor gene expression by RAR agonists, antiestrogen and HER-2/neu antagonist in breast cancer cells. Evidence for a role in apoptosis. *Oncogene* 23: 8135–8145, 2004
21. Zhang H, Ozaki I, Mizuta T, Hamajima H, Yasutake T, Eguchi Y, Ideguchi H, Yamamoto K, Matsuhashi S: Involvement of programmed cell death 4 in transforming growth factor-beta1-induced apoptosis in human hepatocellular carcinoma. *Oncogene* 25: 6101–6112, 2006
22. Wei ZT, Zhang X, Wang XY, Gao F, Zhou CJ, Zhu FL, Wang Q, Gao Q, Ma CH, Sun WS, Fu QZ, Chen YH, Zhang LN: PDCD4 inhibits the malignant phenotype of ovarian cancer cells. *Cancer Sci* 100: 1408–1413, 2009
23. Ruan Q, Wang T, Kameswaran V, Wei Q, Johnson DS, Matschinsky F, Shi W, Chen YH: The microRNA-21-PDCD4 axis prevents type 1 diabetes by blocking pancreatic beta cell death. *Proc Natl Acad Sci U S A* 108: 12030–12035, 2011
24. Liwak U, Thakor N, Jordan LE, Roy R, Lewis SM, Pardo OE, Seckl M, Holcik M: Tumor suppressor PDCD4 represses internal ribosome entry site-mediated translation of antiapoptotic proteins and is regulated by S6 kinase 2. *Mol Cell Biol* 32: 1818–1829, 2012
25. White K, Dempsie Y, Caruso P, Wallace E, McDonald RA, Stevens H, Hatley ME, Van Rooij E, Morrell NW, MacLean MR, Baker AH: Endothelial apoptosis in pulmonary hypertension is controlled by a microRNA/programmed cell death 4/caspase-3 axis. *Hypertension* 64: 185–194, 2014
26. Hilliard A, Hilliard B, Zheng SJ, Sun H, Miwa T, Song W, Göke R, Chen YH: Translational regulation of autoimmune inflammation and lymphoma genesis by programmed cell death 4. *J Immunol* 177: 8095–8102, 2006
27. Dweep H, Sticht C, Kharkar A, Pandey P, Gretz N: Parallel analysis of mRNA and microRNA microarray profiles to explore functional regulatory patterns in polycystic kidney disease: Using PKD/Mhm rat model. *PLoS One* 8: e53780, 2013
28. Pandey P, Qin S, Ho J, Zhou J, Kreidberg JA: Systems biology approach to identify transcriptome reprogramming and candidate microRNA targets during the progression of polycystic kidney disease. *BMC Syst Biol* 5: 56, 2011
29. Ben-Dov IZ, Tan YC, Morozov P, Wilson PD, Rennert H, Blumenfeld JD, Tuschl T: Urine microRNA as potential biomarkers of autosomal dominant polycystic kidney disease progression: Description of miRNA profiles at baseline. *PLoS One* 9: e86856, 2014
30. Pandey P, Brors B, Srivastava PK, Bott A, Boehn SN, Groene HJ, Gretz N: Microarray-based approach identifies microRNAs and their target functional patterns in polycystic kidney disease. *BMC Genomics* 9: 624, 2008
31. Zhong X, Chung AC, Chen HY, Meng XM, Lan HY: Smad3-mediated upregulation of miR-21 promotes renal fibrosis. *J Am Soc Nephrol* 22: 1668–1681, 2011
32. Davis BN, Hilyard AC, Lagna G, Hata A: SMAD proteins control DROSHA-mediated microRNA maturation. *Nature* 454: 56–61, 2008
33. Ribas J, Ni X, Castanares M, Liu MM, Esopi D, Yegnasubramanian S, Rodriguez R, Mendell JT, Lupold SE: A novel source for miR-21 expression through the alternative polyadenylation of VMP1 gene transcripts. *Nucleic Acids Res* 40: 6821–6833, 2012
34. Tan X, Wang S, Zhu L, Wu C, Yin B, Zhao J, Yuan J, Qiang B, Peng X: cAMP response element-binding protein promotes gliomagenesis by modulating the expression of oncogenic microRNA-23a. *Proc Natl Acad Sci U S A* 109: 15805–15810, 2012
35. Gomez IG, MacKenna DA, Johnson BG, Kaimal V, Roach AM, Ren S, Nakagawa N, Xin C, Newitt R, Pandya S, Xia TH, Liu X, Borza DB, Grafals M, Shankland SJ, Himmelfarb J, Portilla D, Liu S, Chau BN, Duffield JS: Anti-microRNA-21 oligonucleotides prevent Alport nephropathy

progression by stimulating metabolic pathways. *J Clin Invest* 125: 141–156, 2015
36. Chau BN, Xin C, Hartner J, Ren S, Castano AP, Linn G, Li J, Tran PT, Kaimal V, Huang X, Chang AN, Li S, Kalra A, Grafals M, Portilla D, MacKenna DA, Orkin SH, Duffield JS: MicroRNA-21 promotes fibrosis of the kidney by silencing metabolic pathways. *Sci Transl Med* 4: 121ra18, 2012
37. Zarjou A, Yang S, Abraham E, Agarwal A, Liu G: Identification of a microRNA signature in renal fibrosis: Role of miR-21. *Am J Physiol Renal Physiol* 301: F793–F801, 2011
38. Rozovski U, Calin GA, Setoyama T, D'Abundo L, Harris DM, Li P, Liu Z, Grgurevic S, Ferrajoli A, Faderl S, Burger JA, O'Brien S, Wierda WG, Keating MJ, Estrov Z: Signal transducer and activator of transcription (STAT)-3 regulates microRNA gene expression in chronic lymphocytic leukemia cells. *Mol Cancer* 12: 50, 2013
39. Thum T, Gross C, Fiedler J, Fischer T, Kissler S, Bussen M, Galuppo P, Just S, Rottbauer W, Frantz S, Castoldi M, Soutschek J, Koteliansky V, Rosenwald A, Basson MA, Licht JD, Pena JT, Rouhanifard SH, Muckenthaler MU, Tuschl T, Martin GR, Bauersachs J, Engelhardt S: MicroRNA-21 contributes to myocardial disease by stimulating MAP kinase signalling in fibroblasts. *Nature* 456: 980–984, 2008
40. Cheng Y, Zhu P, Yang J, Liu X, Dong S, Wang X, Chun B, Zhuang J, Zhang C: Ischaemic preconditioning-regulated miR-21 protects heart against ischaemia/reperfusion injury via anti-apoptosis through its target PDCD4. *Cardiovasc Res* 87: 431–439, 2010
41. Li JH, Liu S, Zhou H, Qu LH, Yang JH: starBase v2.0: Decoding miRNA-ceRNA, miRNA-ncRNA and protein-RNA interaction networks from large-scale CLIP-Seq data. *Nucleic Acids Res* 42: D92–D97, 2014
42. Shillingford JM, Piontek KB, Germino GG, Weimbs T: Rapamycin ameliorates PKD resulting from conditional inactivation of Pkd1. *J Am Soc Nephrol* 21: 489–497, 2010
43. Shillingford JM, Murcia NS, Larson CH, Low SH, Hedgepeth R, Brown N, Flask CA, Novick AC, Goldfarb DA, Kramer-Zucker A, Walz G, Piontek KB, Germino GG, Weimbs T: The mTOR pathway is regulated by polycystin-1, and its inhibition reverses renal cystogenesis in polycystic kidney disease. *Proc Natl Acad Sci U S A* 103: 5466–5471, 2006
44. Zhou X, Fan LX, Sweeney WE Jr., Denu JM, Avner ED, Li X: Sirtuin 1 inhibition delays cyst formation in autosomal-dominant polycystic kidney disease. *J Clin Invest* 123: 3084–3098, 2013
45. Tao Y, Zafar I, Kim J, Schrier RW, Edelstein CL: Caspase-3 gene deletion prolongs survival in polycystic kidney disease. *J Am Soc Nephrol* 19: 749–755, 2008
46. Tao Y, Kim J, Faubel S, Wu JC, Falk SA, Schrier RW, Edelstein CL: Caspase inhibition reduces tubular apoptosis and proliferation and slows disease progression in polycystic kidney disease. *Proc Natl Acad Sci U S A* 102: 6954–6959, 2005
47. Shibazaki S, Yu Z, Nishio S, Tian X, Thomson RB, Mitobe M, Louvi A, Velazquez H, Ishibe S, Cantley LG, Igarashi P, Somlo S: Cyst formation and activation of the extracellular regulated kinase pathway after kidney specific inactivation of Pkd1. *Hum Mol Genet* 17: 1505–1516, 2008
48. Nishio S, Tian X, Gallagher AR, Yu Z, Patel V, Igarashi P, Somlo S: Loss of oriented cell division does not initiate cyst formation. *J Am Soc Nephrol* 21: 295–302, 2010
49. Gresh L, Fischer E, Reimann A, Tanguy M, Garbay S, Shao X, Hiesberger T, Fiette L, Igarashi P, Yaniv M, Pontoglio M: A transcriptional network in polycystic kidney disease. *EMBO J* 23: 1657–1668, 2004
50. Patel V, Li L, Cobo-Stark P, Shao X, Somlo S, Lin F, Igarashi P: Acute kidney injury and aberrant planar cell polarity induce cyst formation in mice lacking renal cilia. *Hum Mol Genet* 17: 1578–1590, 2008
51. Williams SS, Cobo-Stark P, Hajarnis S, Aboudehen K, Shao X, Richardson JA, Patel V, Igarashi P: Tissue-specific regulation of the mouse Pkhd1 (ARPKD) gene promoter. *Am J Physiol Renal Physiol* 307: F356–F368, 2014
52. Shao X, Somlo S, Igarashi P: Epithelial-specific Cre/lox recombination in the developing kidney and genitourinary tract. *J Am Soc Nephrol* 13: 1837–1846, 2002
53. Wu G, D'Agati V, Cai Y, Markowitz G, Park JH, Reynolds DM, Maeda Y, Le TC, Hou H Jr., Kucherlapati R, Edelmann W, Somlo S: Somatic inactivation of Pkd2 results in polycystic kidney disease. *Cell* 93: 177–188, 1998
54. Trapnell C, Pachter L, Salzberg SL: TopHat: Discovering splice junctions with RNA-Seq. *Bioinformatics* 25: 1105–1111, 2009
55. Robinson MD, McCarthy DJ, Smyth GK: edgeR: A Bioconductor package for differential expression analysis of digital gene expression data. *Bioinformatics* 26: 139–140, 2010
56. Trapnell C, Hendrickson DG, Sauvageau M, Goff L, Rinn JL, Pachter L: Differential analysis of gene regulation at transcript resolution with RNA-seq. *Nat Biotechnol* 31: 46–53, 2013

This article contains supplemental material online at http://jasn.asnjournals.org/lookup/suppl/doi:10.1681/ASN.2015060634/-/DCSupplemental.